Assessment of Super-Resolution Ultrasound Imaging Using the Erythrocytes Through Comparison with Micro-CT

Hansen, Lauge Naur; Ráth, Andre; Amin Naji, Mostafa; McDermott, Amy; Sørensen, Charlotte Mehlin; Kjer, Hans Martin; Gundlach, Carsten; Dahl, Anders Bjorholm; Jensen, Jørgen Arendt

Published in:
Proceedings of SPIE

Publication date:
2025

Document Version
Peer reviewed version

Assessment of Super-Resolution Ultrasound Imaging Using the Erythrocytes Through Comparison with Micro-CT

Lauge Naur Hansen[a], Andre Ráth[a], Mostafa Amin-Naji[a], Amy McDermot[d], Charlotte Mehlin Sørensen[d], Hans-Martin Kjer[b], Carsten Gundlach[c], Anders Bjorholm Dahl[b], and Jørgen Arendt Jensen[a]

[a]Center for Fast Ultrasound, Dept. of Health Technology,
[b]3D Imaging Center (3DIM), Dept. of Applied Mathematics and Computer Science,
[c]3D Imaging Center (3DIM), Dept. of Physics,
Technical University of Denmark, Kgs. Lyngby, Denmark
[d]Dept. of Biomedical Sciences, University of Copenhagen, Copenhagen, Denmark

ABSTRACT

This work presents a dual-sample validation study of Super-Resolution Ultrasound imaging using the Erythrocytes (SURE) and state-of-the-art laboratory micro-CT data of rat kidneys. The study hypothesizes that SURE images reliably depict cortical radial blood vessels in rat kidneys, assessed by comparing the depicted blood vessels and vessel diameter estimates from registered micro-CT data. Previous qualitative comparisons between SURE images and micro-CT were either made at an insufficient micro-CT voxel size or in a small region of a rat kidney cortex scanned at a higher resolution. Here, micro-CT data of entire rat kidneys scanned at a voxel size of 5 µm is compared to images from the SURE pipeline with peak detection done after blood flow separation. The separation is achieved using Hankel singular value decomposition before peak detection (SURE-Hankel). The analysis shows a consistent depiction of cortical radial vessels in the entire rat kidney using SURE-Hankel and that these blood vessels have estimated diameters around 50 µm to 100 µm. However, discrepancies in the registered images highlight the need for more accurate CT-to-ultrasound image registration techniques.

Keywords: Super-resolution ultrasound, SURE imaging, phase-contrast CT, blood vessels, rat kidney, imaging comparison, micrometer-scale imaging

1. INTRODUCTION

Advances in diagnostic ultrasound imaging for diseases related to the circulatory system pursue in-depth micro-vascular imaging of whole organs. Currently, other modalities such as computed tomography (CT) perfusion imaging,[1] nuclear imaging,[2] and magnetic resonance imaging[3,4] can depict blood vessels at around millimeter resolution, which restricts imaging of the micro-vascular structure. Ultrasound localization microscopy (ULM) is an ultrasound perfusion technique that accumulates the tracks of gas-filled microbubbles as they travel through the bloodstream to render a super-resolution image of the vascular structure at the micrometer scale.[5–8] A recent contribution to the field of super-resolution ultrasound imaging is a method named Super-Resolution Ultrasound using the Erythrocytes (SURE), which detects the position of received peak signals from moving red blood cells using only a few seconds of data without the need for contrast agent infusion.[9,10]

However, the completeness of blood vessel representation using methods based on ULM or SURE depends on several factors. One aspect is detecting signals from the entire lumen of all vessels, especially signals from slowly moving microbubbles or red blood cells in the microcirculation. Seminal work on ULM validated the imaging results to optical images of superficial blood vessels,[11–14] histochemical microscopy,[15] brightfield microscopy,[14] acoustic angiography,[16] and to micro-CT scans with intravascular contrast.[9,15,17–24] However, as super-resolution ultrasound imaging methods continuously improve the resolution limit of the systems and aim to visualize microvessels and capillaries with diameters down to below 10 µm, optical images cannot be used for validation, nor can previous seminal micro-CT validation because of insufficient resolution. However, it remains essential to validate whether the imaging techniques accurately represent blood vessel morphology and consistently depict blood vessels at the micrometer scale in the ultrasound imaging plane.

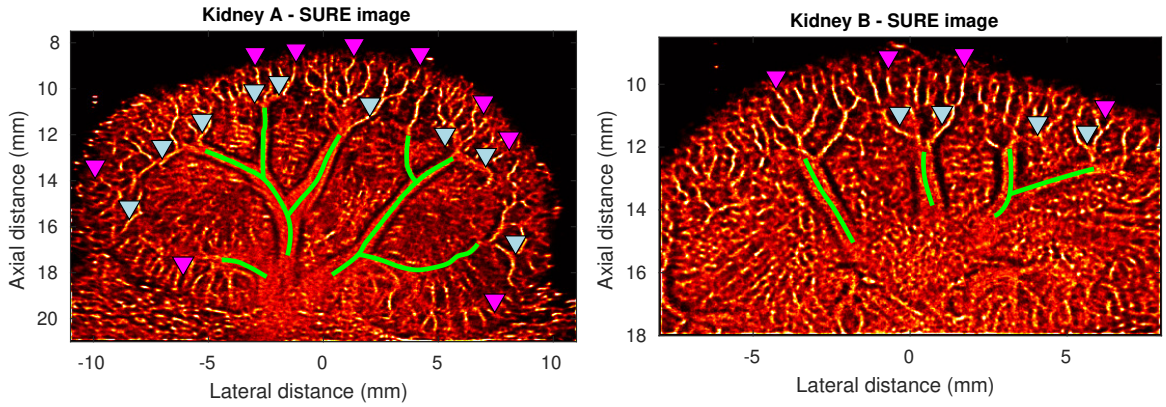

Figure 1. SURE images of two rat kidney samples (3 s of data). Green lines denote interlobar vessels, gray triangles indicate specific examples of arcuate vessels, and purple triangles mark select cortical radial vessels.

Here, unparalleled micro-CT data of rat kidneys from the first commissioned Exciscope Polaris phase contrast micro-tomography scanner (Exiscope AB, Sweden) is used to assess SURE imaging performance. This dual-sample assessment study includes qualitative evaluation of SURE blood vessel detection based on registered micro-CT projection images and blood vessel thickness estimates from the micro-CT volume.

The micro-tomography scanner houses a liquid-metal-jet anode in the X-ray tube (Excillum AB, Sweden) and supports a higher X-ray flux than sources of solid metal. This enables tomographic image quality in a laboratory micro-tomography scanner that would otherwise only be possible at synchrotron facilities. Moreover, the Exciscope Polaris can scan large samples such as an entire rat kidney at a voxel size of 3 µm to 5 µm in two hours, which would require multiple 10-hour long scans to cover in other laboratory scanners and at synchrotron facilities. This is the first validation study of SURE imaging based on unprecedented rat kidney micro-tomography data from the Exciscope Polaris scanner.

The study evaluates images from the SURE pipeline[9] and an axial flow decomposition SURE pipeline using Hankel singular value decomposition for separation of both temporal and spatial variations in the speckle signal (SURE-Hankel). The hypothesis is that SURE images reliably depict blood vessels in the rat kidney cortex with expected diameters in the range of 15 µm to 100 µm.

2. METHODS

Ultrasound scanning was conducted on exposed kidneys from two 40-week Sprague-Dawley rats with a frame rate of 208 Hz using a GE L8-18iD probe connected to a Vantage 256 research scanner operated at a center frequency of 10 MHz using synthetic aperture ultrasound.[25] Data collection for generating the SURE image spanned 3 s, and image formation was done using the SURE pipeline.[9] Flow was separated by axial direction using the positive and negative Fourier spectra of the complex IQ data. Subsequently, blood flow was separated using Hankel matrix singular value decomposition and then subject to peak detection (SURE-Hankel).

In addition, phase-contrast microtomography scans (Exciscope Polaris, Exciscope AB, Sweden) were performed on fixated kidneys, which contained intravascular contrast (Vascupaint™ Silicone Rubber Injection Compounds, MediLumine, Inc., Canada) prepared with 2 mL yellow silicone, 3 mL dilutant, and 0.25 mL catalyst which constitutes 4.76 % of the total volume, and otherwise as previously described.[26] The peak intensity of the X-ray spectrum was 70 kV with a source power of 131 W. The effective X-ray propagation distances were 137.08 mm and 136.99 mm, and the voxel sizes were 5.45 µm and 4.64 µm for kidney A and B respectively. The duration of each CT scan was 2 h 12 min.

The 2D SURE imaging plane was manually co-registered to the CT volume using Dragonfly software (v2024.1, Comet Technologies Canada Inc., Montreal, Canada) by comparing the SURE image to maximum intensity projections of oblique, planar cut-planes over 1 mm to 1.5 mm of the CT volume, respectively. The

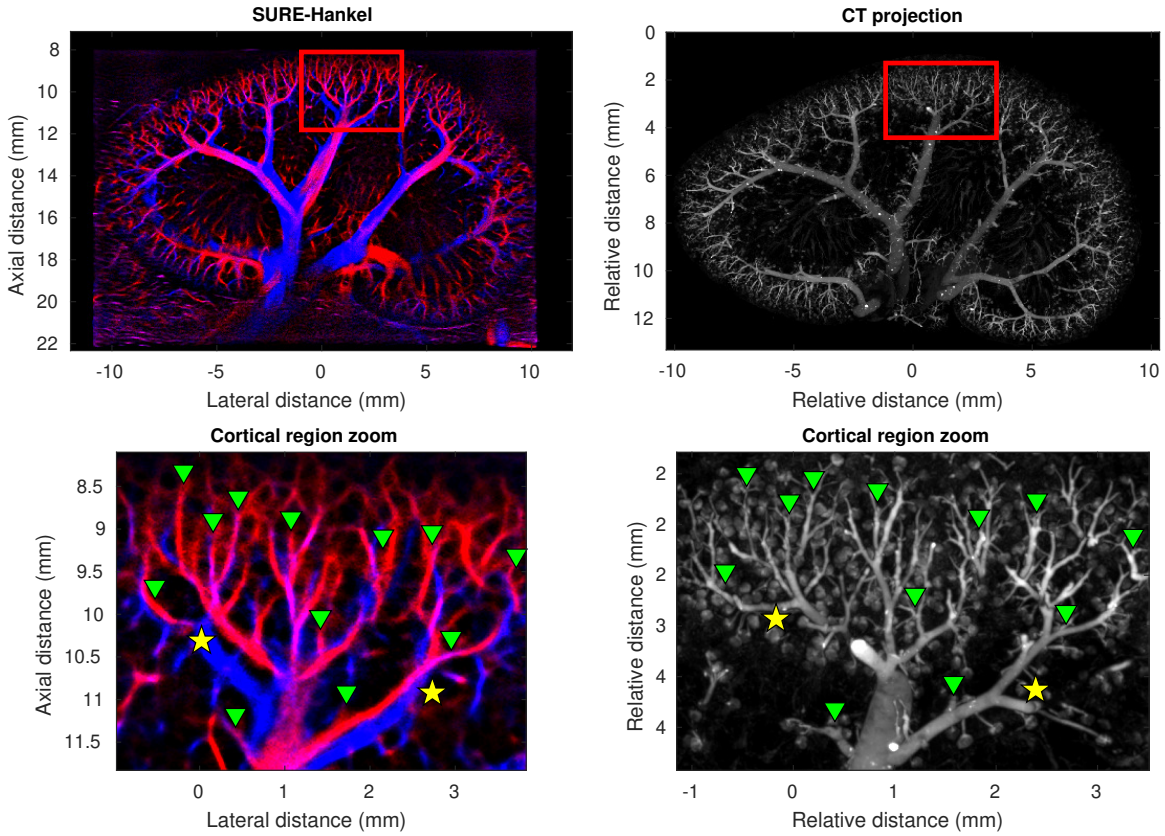

Figure 2. SURE-Hankel and micro-CT projection images of rat kidney sample A. Upper panel: entire kidney with a red square indicating the zoomed region in the lower panel. In SURE-Hankel images, red/blue indicate upward/downward axial flow. CT values show a mix of absorption and phase shift. Green triangles mark corresponding vessels; yellow stars mark discrepancies in the cortex. CT projection shows glomeruli in the cortex.

CT projections were computed over a constant thickness over the projected direction, thus not taking varying elevation focus for different parts of the SURE images into account.

Blood vessel size measurements were based on manually selected intensity threshold masks for blood vessels in the CT volumes. The masks were convolved with a Gaussian kernel with a standard deviation of half the assumed 20 µm spatial resolution of the CT volume, and blood vessel diameter measurements were made on this mask in Python using the localthickness package.[27] For SURE-Hankel images, full-width at half-maximum (FWHM) values of line profiles through selected blood vessels were computed in MATLAB (v24.2 R2024b, The MathWorks Inv., Natick, Massachusetts, United States)

3. RESULTS

The SURE images from both kidneys depict interlobar, arcuate, and cortical radial blood vessels (see annotated SURE images in Fig. 1). In particular, the SURE images of kidneys A and B display three and two interlobar blood vessels originating from the hilum, respectively (compare SURE images in Fig. 1 and CT images in Figs. 2 and 3). Arcuate vessels connected to these interlobar vessels are visible in both SURE images and many cortical radial vessels are also depicted.

However, speckle signals from overlapping arteries and veins may contribute to depicting one vessel structure in the SURE images. Embedding axial flow direction in the SURE images reveals whether a vein, an artery, or separate vessels with different axial flow directions contribute to a depicted vessel structure. Indeed, the SURE-depicted interlobar blood vessels and blood vessels in the cortical region contain signals from both

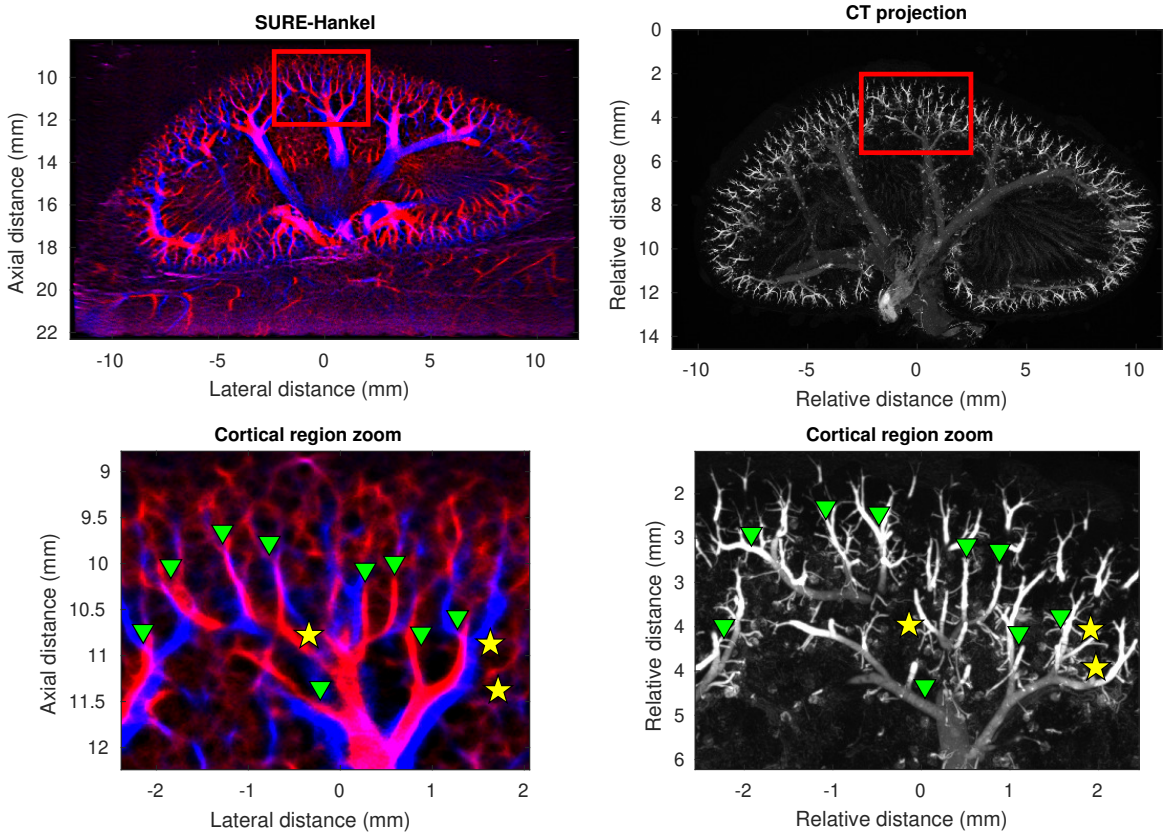

Figure 3. SURE-Hankel and micro-CT images of rat kidney sample B. Upper: entire kidney with a red square for the zoomed region in the lower panel. SURE-Hankel: red/blue for upward/downward flow. CT values combine absorption and phase shift. Green triangles: corresponding cortical vessels; yellow stars: cortical discrepancies.

arteries and veins (compare SURE images in Fig. 1 to SURE-Hankel images in Figs. 2 and 3). Along with the interlobar vessels, the SURE-Hankel images and their registered micro-CT projection images depict matching arcuate vessels and many cortical radial vessels (see green triangles in Figs. 2 and 3). The micro-CT projections mainly include arteries because the contrast agent did not solidify in the veins. This may explain the absence of particular veins in the CT projection images (e.g., see yellow stars in Fig. 2). But it may also indicate a displacement in the registration relative to the ultrasound focus plane or that the elevation focus span is underestimated for the CT projection (e.g., see leftmost yellow star in Fig. 3).

The expected diameter of cortical radial vessels is between 15 µm to 100 µm, and this vessel type is depicted in the SURE-Hankel images (see Figs. 2 and 3). From the CT image, the measured vessel diameters in the kidney cortex is also within the expected range. However, besides the cortical radial vessels, the CT projection image of kidney A displays many arterioles and glomerular vessels, which are absent in the SURE-Hankel images (see Fig. 2). Interestingly, fewer glomerular vessels are depicted in the CT projection image of kidney B even though arterioles are visible (see Fig. 3).

FWHM values from line profiles across selected blood vessels are between 56 µm to 90 µm and 52 µm to 70 µm in kidneys A and B, respectively. Blood vessel diameter measurements from the CT-derived blood vessel masks show thicknesses for the same vessels between 93 µm to 124 µm and 60 µm to 146 µm in kidney A and B, respectively (see rightmost plots in Figs. 4 and 5).

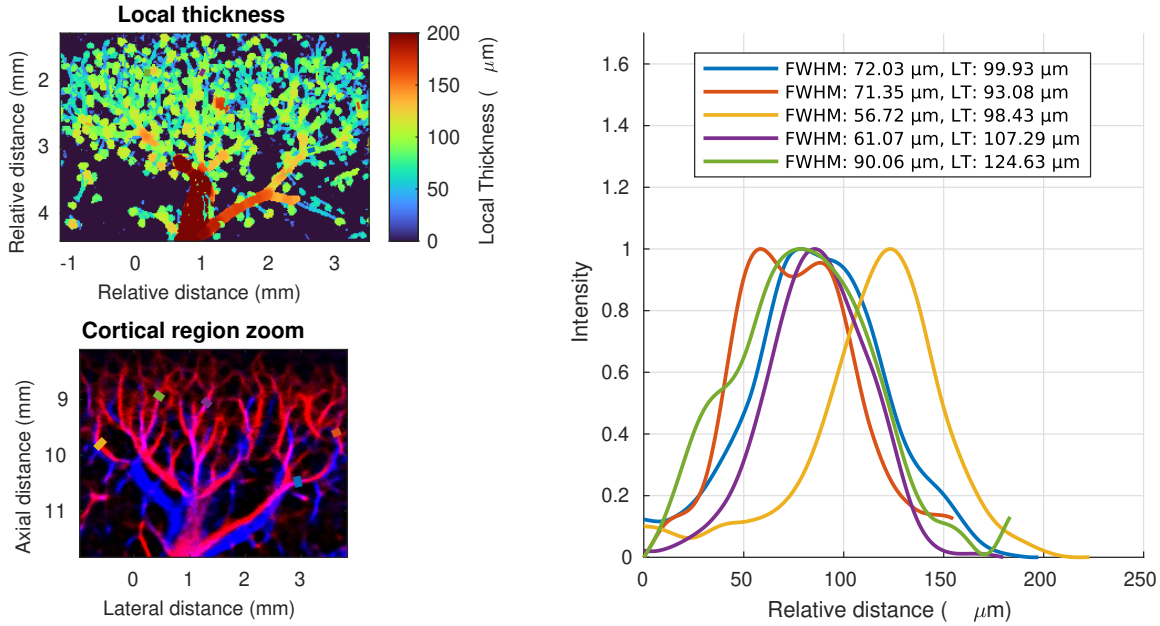

Figure 4. These plots relate to kidney A. (Upper left) Local thickness (LT) image derived from CT data, displaying variations in cortical blood vessel diameters. Five overlaid line segments indicate blood vessels where the maximum local thickness or diameter is reported. The color bar represents local thickness values in micrometers with a display range of 0 µm to 200 µm. (Lower left) SURE-Hankel image showing vascular structures with overlaid line profiles. The profiles are used to compute full-width at half-maximum (FWHM) values, which quantify vessel widths based on signal intensity. (Right) Line profile plots displaying normalized intensity variations along the selected vessel segments. The legend lists the computed FWHM and LT values for each profile, allowing direct comparison between structural thickness from CT and vessel width estimations from SURE-Hankel imaging.

4. DISCUSSION

The present study evaluates the ability of Super-Resolution Ultrasound using the Erythrocytes (SURE) to depict blood vessels in rat kidneys, using high-resolution micro-CT as a reference modality. The findings indicate that SURE, particularly with Hankel singular value decomposition (SURE-Hankel), successfully visualizes interlobar, arcuate, and cortical radial vessels. However, discrepancies between the two modalities highlight both methodological challenges and areas for future improvement.

The vessel diameter measurements obtained from SURE-Hankel images generally align with the micro-CT projections, particularly for cortical radial vessels, where vessel diameters ranged from approximately 10 µm to 100 µm. However, compared to micro-CT, there is a consistent trend of smaller vessel diameters in SURE-Hankel FWHM measurements. Several factors may contribute to this: 1) Echo-cancellation crop scatterers below some velocity threshold, which means only flow in the middle of the blood vessel may be detected. 2) The ultrasound localization method detects peak intensity signals, which may bias vessel width estimates toward the highest flow regions rather than the entire vessel lumen. 3) FWHM does not strictly correspond to vessel size because of dependency on the noise floor, detection sensitivity, and smoothing. 4) Infusion of CT contrast agent in the excised kidney may expand the arteries due to pressure increase. 5) The simple intensity threshold segmentation on the CT volume may cause incomplete segmentation of the blood vessel lumen due to uneven contrast agent distribution, perfusion and low signal-to-noise ratio in vessels with low intensity. Hence, it may be that discrepancies in blood vessel size measurements between the two modalities result from the ultrasound imaging scheme and CT sample preparation, which again highlights the inherent difficulty in validating super-resolution ultrasound methods against other modalities such as micro-CT.

Moreover, the inability to visualize veins in the micro-CT images due to incomplete contrast perfusion limits the validation process. Since the contrast agent did not solidify within the venous system, the CT

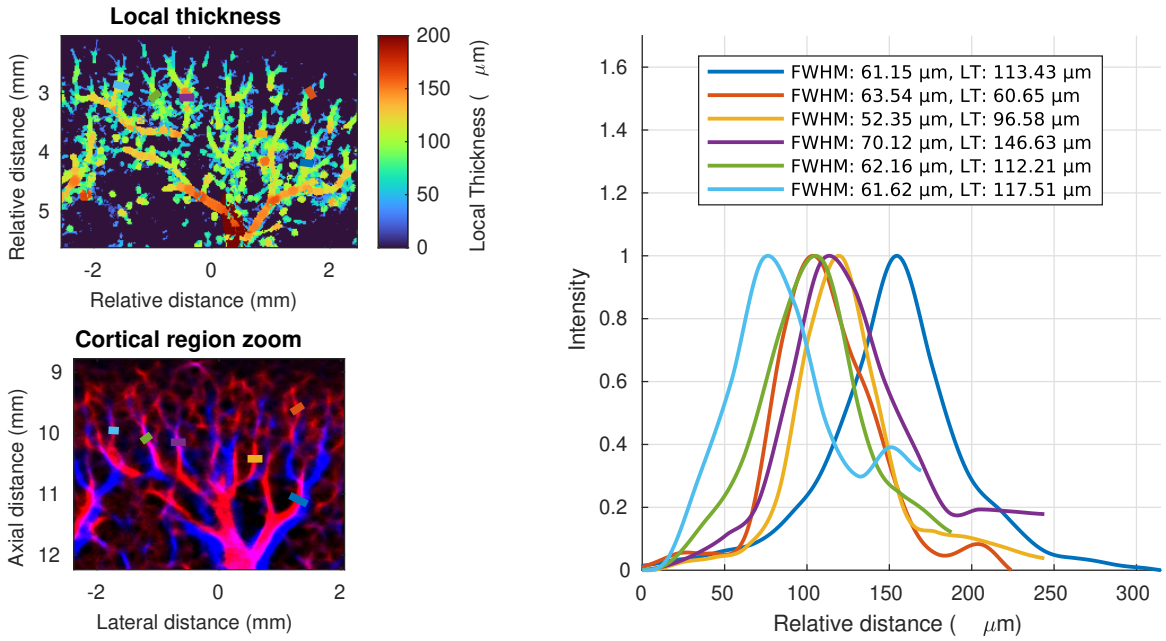

Figure 5. These plots pertain to kidney B. (Top left) The local thickness (LT) image shows variations in cortical blood vessel diameters. The image is overlaid with line segments that mark vessel locations where the maximum local thickness is measured. The color bar represents the thickness values in micrometers with a display range of 0 µm to 200 µm. (Bottom left) The SURE-Hankel image shows vascular structures with superimposed line profiles, which are used to determine the full width at half-maximum (FWHM). (Right) Line profile plots depict normalized intensity variations along the segmented vessels. The legend presents each profile's computed FWHM and LT values, facilitating a comparison between CT-derived thickness measurements and SURE-Hankel vessel width estimates.

projections primarily depict arteries. This makes it difficult to assess how well SURE-Hankel differentiates between arteries and veins and whether the observed structures in ultrasound correspond to both vessel types. However, the qualitative assessment of the SURE-Hankel imaging performance compared to CT maximum intensity projections showcases the ability of SURE imaging to depict cortical radial blood vessels in the rat kidney (see Figs. 2 and 5.

The registration of SURE-Hankel images to micro-CT projections was performed manually, introducing potential alignment errors. Since SURE imaging detects moving scatterers within an ultrasound beam and projects detections onto a 2D plane and micro-CT provides an isotropic volumetric dataset, co-registering these modalities is inherently challenging. In addition, the pixel and voxel intensities in SURE and CT images correspond to flow in SURE images and a combination of absorption and phase shift in the CT volumes. Hence, there is an expected degree of discrepancy between CT maximum intensity projections and SURE images. In addition, micro-CT scanning was performed on fixated kidneys, which introduces potential tissue shrinkage or deformation and may alter vessel morphology. This may contribute to some of the observed discrepancies in vessel depiction between the modalities beyond rigid co-registration inaccuracy.

5. CONCLUSION

In this dual-sample assessment of SURE and SURE-Hankel imaging performance, corresponding micro-CT projection images were co-registered with the ultrasound images of entire rat kidneys. The analysis shows microvessels in the SURE-Hankel images comparable to those of the CT projection images. The depicted blood vessels range from the large interlorbar vessels to cortical radial vessels with CT-derived diameters between 25 µm to 100 µm. Furthermore, cortical radial vessels in the SURE-Hankel images have measured diameters within the expected range for those blood vessels. The vessel widths were reported by FWHM values for the SURE-Hankel images and local thickness for the CT volume. SURE-Hankel images differentiate blood vessels

with upwards and downwards flow, but the CT projection images mainly display arteries due to issues with contrast agent perfusion. Even though the SURE-Hankel and CT projection images mostly display similar vessel structures, the inability to include most veins in the CT images precludes validating the depiction of veins.

ACKNOWLEDGMENTS

The European Research Council (ERC) Synergy Grant no. 854796 funds the work.

REFERENCES

[1] Miles, K. A., "Measurement of tissue perfusion by dynamic computed tomography," *Brit. J. Radiol.* **64**(761), 409–412 (1991).

[2] Underwood, S. R., Anagnostopoulos, C., Cerqueira, M., Ell, P. J., Flint, E. J., Harbinson, M., Kelion, A. D., Al-Mohammad, A., Prvulovich, E. M., Shaw, L. J., and Tweddel, A. C., "Myocardial perfusion scintigraphy: The evidence," *Eur. J. Nucl. Med. Mol. Imaging* **31**(2), 261–291 (2004).

[3] Williams, D. S., Detre, J. A., Leigh, J. S., and Koretsky, A. P., "Magnetic resonance imaging of perfusion using spin inversion of arterial water," *Proc. Natl. Acad. Sci. U.S.A.* **89**(1), 212–216 (1992).

[4] Padhani, A. R., "Dynamic contrast-enhanced MRI in clinical oncology: Current status and future directions," *J. Magn. Reson. Imaging* **16**(4), 407–422 (2002).

[5] Couture, O., Tanter, M., and Fink, M., "Method and device for ultrasound imaging," *Patent Cooperation Treaty (PCT)/FR2011/052810* (2010).

[6] Couture, O., Besson, B., Montaldo, G., Fink, M., and Tanter, M., "Microbubble ultrasound super-localization imaging (MUSLI)," in [*Proc. IEEE Ultrason. Symp.*], 1285–1287 (2011).

[7] Siepmann, M., Schmitz, G., Bzyl, J., Palmowski, M., and Kiessling, F., "Imaging tumor vascularity by tracing single microbubbles," *Proc. IEEE Ultrason. Symp.* , 6293297, 1906–1908 (2011).

[8] Viessmann, O. M., Eckersley, R. J., Christensen-Jeffries, K., Tang, M. X., and Dunsby, C., "Acoustic super-resolution with ultrasound and microbubbles," *Phys. Med. Biol.* **58**, 6447–6458 (2013).

[9] Jensen, J. A., Naji, M. A., Præsius, S. K., Taghavi, I., Schou, M., Hansen, L. N., Andersen, S. B., Sørensen, C. M., Nielsen, M. B., Gundlach, C., Kjer, H. M., Dahl, A., Tomov, B. G., Ommen, M., and Thomsen, E. V., "Super-resolution ultrasound imaging using the erythrocytes—Part I: Density images," *IEEE Trans. Ultrason. Ferroelec. Freq. Contr.* , 1–20 (2024).

[10] Naji, M. A., Taghavi, I., Schou, M., Præsius, S. K., Hansen, L. N., Andersen, S. B., Søgaard, S. B., Pandru, N., Nielsen, M. B., Kjer, H. M., Tomov, B. G., Dahl, A. B., Sørensen, C. M., and Jensen, J. A., "Super-resolution ultrasound imaging using the erythrocytes—Part II: Velocity images," *IEEE Trans. Ultrason. Ferroelec. Freq. Contr.* (2024).

[11] Christensen-Jeffries, K., Browning, R. J., Tang, M., Dunsby, C., and Eckersley, R. J., "In vivo acoustic super-resolution and super-resolved velocity mapping using microbubbles," *IEEE Trans. Med. Imag.* **34**(2), 433–440 (2015).

[12] Tang, S., Song, P., Trzasko, J. D., Lowerison, M., Huang, C., Gong, P., Lok, U., Manduca, A., and Chen, S., "Kalman filter–based microbubble tracking for robust super-resolution ultrasound microvessel imaging," *IEEE Trans. Ultrason. Ferroelec. Freq. Contr.* **67**(9), 1738–1751 (2020).

[13] Huang, C., Lowerison, M. R., Trzasko, J. D., Manduca, A., Bresler, Y., Tang, S., Gong, P., Lok, U., Song, P., and Chen, S., "Short acquisition time super-resolution ultrasound microvessel imaging via microbubble separation," *Scientific Reports* **10**(1), 6007 (2020).

[14] Ozdemir, I., Johnson, K., Mohr-Allen, S., Peak, K. E., Varner, V., and Hoyt, K., "Three-dimensional visualization and improved quantification with super-resolution ultrasound imaging-validation framework for analysis of microvascular morphology using a chicken embryo model," *Phys. Med. Biol.* **66**(8), 085008 (2021).

[15] Chen, Q., Yu, J., Lukashova, L., Latoche, J. D., Zhu, J., Lavery, L., Verdelis, K., Anderson, C. J., and Kim, K., "Validation of ultrasound super-resolution imaging of vasa vasorum in rabbit atherosclerotic plaques," *IEEE Trans. Ultrason. Ferroelec. Freq. Contr.* **67**(8), 1725–1729 (2020).

[16] Lin, F., Shelton, S. E., Espindola, D., Rojas, J. D., Pinton, G., and Dayton, P. A., "3-D ultrasound localization microscopy for identifying microvascular morphology features of tumor angiogenesis at a resolution beyond the diffraction limit of conventional ultrasound," *Theranostics* **7**(1), 196–204 (2017).

[17] Opacic, T., Dencks, S., Theek, B., Piepenbrock, M., Ackermann, D., Rix, A., Lammers, T., Stickeler, E., Delorme, S., Schmitz, G., and Kiessling, F., "Motion model ultrasound localization microscopy for preclinical and clinical multiparametric tumor characterization," *Nat. comm.* **9**(1), 1527:1–13 (2018).

[18] Zhu, J., Rowland, E. M., Harput, S., Riemer, K., Leow, C. H., Clark, B., Cox, K., Lim, A., Christensen-Jeffries, K., Zhang, G., Brown, J., Dunsby, C., Eckersley, R. J., Weinberg, P. D., and Tang, M.-X., "3D super-resolution US imaging of rabbit lymph node vasculature in vivo by using microbubbles," *Radiology* **291**(3), 642–650 (2019).

[19] Andersen, S. B., Taghavi, I., Kjer, H. M., Søgaard, S. B., Gundlach, C., Dahl, V. A., Nielsen, M. B., Dahl, A. B., Jensen, J. A., and Sørensen, C. M., "Evaluation of 2D super-resolution ultrasound imaging of the rat renal vasculature using ex vivo micro-computed tomography," *Scientific Reports* **11**(1), 24335 (2021).

[20] Chabouh, G., Denis, L., Bodard, S., Lager, F., Renault, G., Chavignon, A., and Couture, O., "Whole organ volumetric sensing ultrasound localization microscopy for characterization of kidney structure," *IEEE Trans. Med. Imag.* **PP**(99), 1–1 (2024).

[21] Chavignon, A., Heiles, B., Hingot, V., Orset, C., Vivien, D., and Couture, O., "3D transcranial ultrasound localization microscopy in the rat brain with a multiplexed matrix probe," *IEEE Trans. Biomed. Eng.* **69**(7), 2132–2142 (2022).

[22] Hansen, L. N., Kjer, H. M., Amin-Naji, M., Panduro, N. S., Sørensen, C. M., Gundlach, C., Dahl, A. B., and Jensen, J. A., "Comparison of 2D SURE and 3D CT imaging of cortical vessels in a rat kidney," *Proc. IEEE Ultrason. Symp.* (2023).

[23] Demené, C., Robin, J., Dizeux, A., Heiles, B., Pernot, M., Tanter, M., and Perren, F., "Transcranial ultrafast ultrasound localization microscopy of brain vasculature in patients," *Nature Biomedical Engineering* **5**(3), 219–228 (2021).

[24] Denis, L., Bodard, S., Hingot, V., Chavignon, A., Battaglia, J., Renault, G., Lager, F., Aissani, A., Hélénon, O., Correas, J., and Couture, O., "Sensing ultrasound localization microscopy for the visualization of glomeruli in living rats and humans," *Ebiomedicine* **91**, 104578 (2023).

[25] Jensen, J. A., Tomov, B. G., Haslund, L. E., Panduro, N. S., and Sørensen, C. M., "Universal synthetic aperture sequence for anatomic, functional and super resolution imaging," *IEEE Trans. Ultrason. Ferroelec. Freq. Contr.* **70**(7), 708–720 (2023).

[26] Søgaard, S. B., Andersen, S. B., Taghavi, I., Hoyos, C. A. V., Christoffersen, C., Hansen, K. L., Jensen, J. A., Nielsen, M. B., and Sørensen, C. M., "Super-resolution ultrasound imaging provides quantification of the renal cortical and medullary vasculature in obese Zucker rats: A pilot study," *Diagnostics* **12**(7), 1626 (2022).

[27] Dahl, V. and Dahl, A. B., "Fast local thickness," in [*Proceedings of the IEEE/CVF Conference on Computer Vision and Pattern Recognition Workshops*], 4335–4343 (2023).